

Optimized Design of Magnetic Components in Plasma Cutting Power Supply Employing Buck DC-DC Converter

JIANG JIAN-FENG¹, ZHU BIN-RUO¹, YANG XI-JUN², ZHAO WEI-NA², TANG HOU-JUN²

¹ Electric Power Science Research Institute, ² Dept. of electrical engineering

¹ Shanghai Electric Power Company, State Grid, ² Shanghai Jiao Tong University

¹ Shanghai China 200437, ² Shanghai China 200240

¹ P. R. CHINA, ² P. R. CHINA

¹ 247721794@qq.com, ² wnzhaol992@126.com

Abstract: - As for high air power plasma cutting power supply, the employed chopper type DC-DC converter needs to adopt two kinds of magnetic components, including mains frequency step-down phase-shifting transformer (Hereinafter referred to as power transformer) and smoothing reactors. Because the power level is larger and the design needs to be optimized, the resultant total losses of magnetic components will reach several kilowatts or more, which seriously affects the overall conversion efficiency. The countermeasure is to select efficient magnetic materials and optimize design and manufacturing technique. Meanwhile, it is needed to modify the topology of chopper type DC-DC converter and design appropriate switching frequency multiplication modulation algorithm. In this paper, at first, a double Buck DC-DC converter in parallel with respective dual power switches is employed, in which by using the trapezoidal carrier phase shift driving, the output current ripple frequency multiplied by four times at any duty ratio can be obtained, thereby as can reduce the size and heating of smoothing reactors, leading to high precision cutting current and improved workpiece cutting quality. Secondly, the core losses of different magnetic materials are compared and analyzed, so are the structure of smoothing reactor and step-down phase-shifting transformer, winding arrangement and conductor type. On the above basis, the optimization design procedure of the power transformer and smoothing reactor is put forward, the optimal design is picked up from lots of candidates, which brings about less size and loss as well as high conversion efficiency of the plasma cutting power supply. Finally, a smoothing reactor with 1mH inductance and 20kHz switching frequency and a power transformer with thin oriented silicon steel sheet and flat aluminum wire and fabricated and tested within the production-ready plasma cutting machine, which features maximum output current of 270A, the output voltage of 150V and the maximum input power of 45kW. The measured results are satisfactory, including the quality of cutting current and the quality of the cut workpiece approaching the minimum level of laser cutting. It is proved that the proposed switching frequency multiplication modulation algorithm and magnetic design optimization method utilized in chopper type plasma cutting power supply are effective and feasible.

Key-Words: -Plasma cutting power supply, Buck DC-DC converter, Trapezoidal carrier phase-shifting driving, switching frequency multiplication modulation, Step-down transformer, Smoothing reactor

1 Introduction

Known as steel tailor, cutting and welding has become the key technology in the field of bridges, buildings, machinery, ships, aircraft, railway, metallurgy, power generation equipment industry, the development of modern industry can't do without cutting device. With the development of international economy, it needs to vigorously implement the "to cast" principle, which makes the total amount of metal plate cutting materials increased year by year, the required cutting quality and cutting efficiency are also getting higher and higher [1-4]. At present, the metal thermal cutting methods mainly include flame cutting, plasma cutting and laser cutting. The flame cutting has demerits of low speed, rough cutting surface, inferior cutting precision. Laser cutting has merits of high

speed and excellent cutting quality, but the initial investment and operating expenses are not afforded. Plasma cutting can achieve faster speed, better cutting quality and high power level, and its overall cost is lower, which is a promising and advantageous cutting machine.

From the beginning of the 1960's, with the development of power electronic semiconductor devices, plasma cutting technology has made continuous and rapid progress, and rectifier based power supply has experienced from the past silicon rectifier and thyristor rectifier to the modern chopper type and inverter type plasma cutting power supply [5-6]. As for the chopper type plasma cutting power supply, it is characteristic of simple control circuit, high switching frequency, high reliability, good controllability, so that it is commonly used in the

production of more than 20kW plasma cutting power supply, ideal for the high power plasma cutting applications [7-8].

As for plasma cutting power supply, there are lots of practical considerations, such as how to design arc-pilot transformer[9], system control strategy[10], power switch design[11] and protection design[12]. In addition, as the major passive components, the step-down phase-shifting transformer and smoothing reactor design should be optimized according to the infinite element analysis[13-15], loss model[16-24] and planar inductance design[25].

In the chopper type plasma cutting power supply, high power magnetic components are needed, such as smoothing reactor and 380V/220V mains frequency step-down phase-shifting transformer (Hereinafter referred to as power transformer). Due to the high power and high current level, the losses of magnetic components will reach a few kilowatts or more, which has a serious impact on the power conversion efficiency of plasma cutting power. In the smoothing reactor design, the loss is mainly decided by the core material and wire type. In power transformer design, it additionally need to consider the structure and connection of transformer windings and to adopt the necessary cooling method.

In view of the fact that connected with the power grid, the volume and loss of power transformer can be reduced only by optimizing the employed material and selected structure. For the smoothing reactor, in order to reduce the volume and weight, but to maintain the current accuracy, it needs to increase the equivalent ripple frequency, it is necessary to improve the switching frequency. However merely increasing the switching frequency will make the switching loss increased dramatically and make aggravate the difficulty of heat treatment. In order to solve this problem, a new power circuit and the corresponding modulation algorithm are needed.

In this paper, from the point of view of a practical 45kW chopper type plasma cutting power supply, to design optimally power transformer and smoothing reactor, aiming to reduce their volume and loss and to improve the efficiency. In chapter II, the topology and principle of the chopper type plasma cutting power supply is briefly introduced, and the trapezoidal carrier

phase-shifting modulation algorithm is also described for two Buck DC-DC converters in parallel with respective two power switches. In chapter III, for proper selection of appropriate material and structure, the influence of different magnetic materials, transformer structure, winding arrangement and conductor structure on magnetic element characteristics are analyzed and compared. In chapter IV, the design process of power transformer and smoothing reactor are given, and the optimal design scheme is picked up from several candidates. In chapter V, the satisfactory experimental results is provided.

2 Principle of chopper type plasma cutting power supply

2.1 Selection of topology

The topology of Buck DC-DC converter is shown in Fig.1, where through the step-down power frequency transformer, the reduced three-phase AC mains is rectified and filtered, and then through the power switch chopping, the pulse voltage is obtained, and also then through the LC filtering, the stable DC current is output and the plasma arc column is formed.

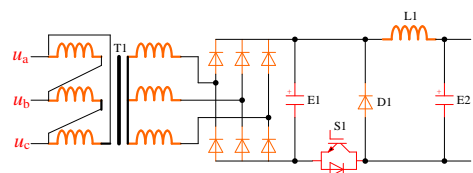


Fig.1 Chopper type plasma cutting power supply

In Fig.1, IGBT S1 and freewheeling diode D1 is one power device, which can be derived from an bridge-arm of IGBT power module, but the gate of the high-end IGBT should be always blocked without any triggering.

Because the input power of the concerning plasma cutting power supply is 45kW, two Buck DC-DC converter output connected in parallel at output, in the sharing of system power capacity at any time, which can reduce the current stress of the switches and improve the stability of the power system.

After the comprehensive consideration, the power circuit shown in Fig.2 is employed as the plasma cutting power supply circuit, where the part "1" stands for the first Buck DC-DC converter, including two pairs of anti-parallel IGBTs and freewheeling diodes,

namely S1 and D1, S2 and D2, input with a DC voltage u_{i1} and output with a DC current i_{L1} . Part "2" in Fig.2 stands for the second Buck DC-DC converter, including two pairs of anti-paralleled IGBTs and freewheeling diodes, namely S3 and D3, S4 and D4, input with a DC voltage u_{i2} and output with a DC current i_{L2} . And part "1" in Fig.2 stands for the second Buck DC-DC converter. Part "3" stands for the power transformer with two secondary windings of WYE connection and DELTA connection. And part "4" stands for the workpiece, cutting torch and arc ignition device. The synthesized i_{L1} and i_{L2} is the output cutting current i_o , which is adjustable continuously within the range from tens of amperes to 260A, according to the type and thickness of the workpiece.

When the maximum output current is less than 130A, only one of the two Buck DC-DC converters operates. And when the output current required is greater than 130A, the two Buck DC-DC converters operates at the same time.

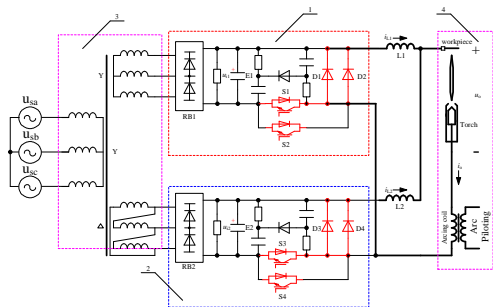


Fig.2 Two channel paralleled plasma cutting power supply

2.2 Selection of modulation algorithm

As for the chopping type plasma cutting power supply, the input DC voltage of 300V or so, the output DC voltage is about 150V, so the maximum duty cycle is about 0.5. There are two feasible modulation algorithms, depicted as follows.

Method 1: S1 and S2 are triggered by phase-shifting of half switching period, so are S3 and S4, and S1 and S3 are also triggered by phase-shifting of 1/4 switching period, the duty ratios of S1, S2, S3 and S4 are equal to the total duty ratio, then the output current ripple frequency will be increased by four times, but this is only applicable when the total duty ratio is less than 0.5.

Method 2: S1 and S2 are triggered by phase-shifting of half switching period, so are S3 and

S4, and S1 and S3 are also triggered by phase-shifting of 1/4 switching period, the duty ratios of S1, S2, S3 and S4 are equal to half of the total duty ratio, then the output current ripple frequency will be increased by four times no matter how much the total duty ratio is. In this case, the carrier turns out to be trapezoidal waveform, and the modulation algorithm is shown in Fig. 3.

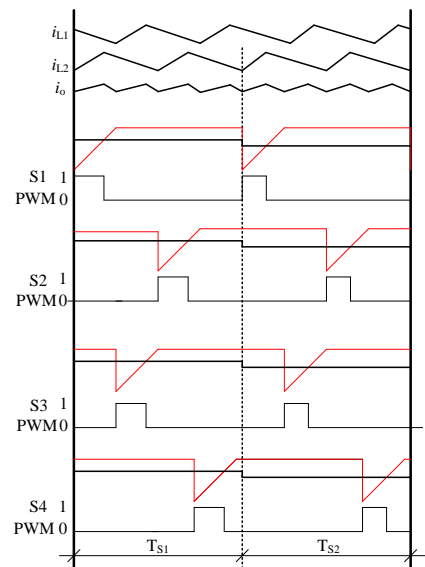


Fig. 3 Driving timing of the four power components

Output current closed loop control strategy, PI control strategy as well as democratic current-sharing strategy are utilized in the plasma cutting power supply using, as shown in Fig. 4. The reference of the output current of each DC-DC Buck converter is half of the total output current. In order to eliminate the static error and improve the dynamic performance, the variable speed PI regulator is introduced. According to the deviation of current magnitude and direction, the proportion coefficient and integral coefficient varies accordingly, which is consistent with the output characteristics of the plasma cutting power supply.

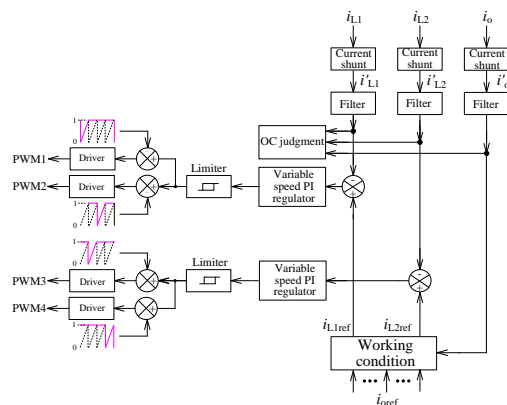


Fig. 4 Control diagram of the plasma cutting power supply

3 Optimization of magnetic materials and structures

3.1 Magnetic materials

For the high power supply, the magnetic components are the essential devices and bear the energy transfer, storage and filtering effect. The volume and the weight generally accounted for 20% to 30% of the whole power supply. The total loss accounted for about 30%, composed of hysteresis loss P_h , eddy current loss P_e and residual loss P_c , which are mainly affected by lots of factors such as magnetic material, operating frequency, AC magnetic flux density, wave shape, and so on.

The magnetic core loss can be calculated by the Steinmetz formula under the sine excitation:

$$P = K \cdot f_s^\alpha \cdot B_{ac}^\beta \quad (1)$$

where K , α and β are core factors, related to the core working conditions, which can be obtained by reference to datasheet from core manufacturers or through self-testing and curve fitting.

The calculation of magnetic core loss under non sinusoidal excitation can be separated from the empirical formula or based on Fourier series decomposition.

For smoothing reactor, according to core types, it can be divided into single magnetic material reactor and mixed magnetic material.

The former core material can adopt high permeability material with air gap or powder magnetic core, and the latter core material can adopt magnetic material mixed with high or low permeability, or magnetic material mixed with high permeability and permanent material.

The above four kinds of magnetic materials are compared in terms of volume, cost, loss and inductance, as shown in Table 1. In the paper, the magnetic material with high permeability and air gap is selected to design the structure of the smoothing reactor.

3.2 Structure of power transformer

Due to presence of three-phase rectifier in the chopper type plasma cutting power supply and its strong nonlinearity and time varying property, the rectifier circuit will produce serious harmonic pollution in power system and arouse deteriorated

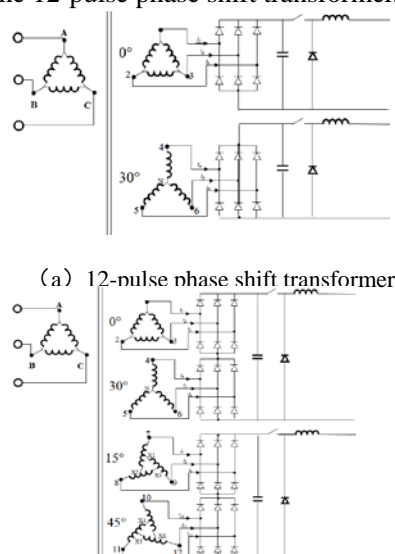
power factor of the power grid, leading to voltage and current distortion as well as the adverse impact on other electricity consumers. Phase shifting transformer can be designed with increased pulse number on its primary side to reduce the harmonic content, which has the advantages of simple structure, high reliability, which is suitable for high current power supply, high voltage inverter and HVDC transmission system.

The design of phase shift transformer in plasma cutting power supply can be divided into two kinds: 12-pulse phase shift transformer and 24-pulse phase shift transformer, as shown in Fig. 5.

The 12-phase pulse transformer has the advantages of simple structure and easy fabrication, but the mains side current total harmonic distortion is a little large, and THD_i is 15.22%. The power factor is $0.9886 \cdot \cos\alpha$, of which the displacement factor is $\cos\alpha$, the distortion factor is 0.9886.

The 24-pulse phase shifting transformer has complex winding and wiring, the mains side current total harmonic distortion is small, and THD_i is 7.5%, the power factor is $0.9971 \cdot \cos\alpha$, of which the displacement factor is $\cos\alpha$, and the distortion factor is 0.9971.

As for the two kinds of phase shift transformers, the wire specification, coil and magnetic core material consumption are the same, but the 24-pulse phase shift transformer winding is not cost-effective. By comprehensive comparison, it seems reasonable to employ the 12-pulse phase shift transformer.



(a) 12-pulse phase shift transformer
(b) 24-pulse phase shift transformer
Fig.5 Design of power transformer

3.3 Winding arrangement of power transformer

The transformer winding arrangement is shown in Fig. 6, where "P" stands for the primary-side winding, and "S" is the secondary-side winding. "*" indicates the direction of current, flowing in vertically, "." indicates the direction of current, flowing out vertically. "H" indicates the magnetic field strength.

The shown in Fig.6 (a) is the traditional structure, where the magnetic field strength of the primary winding will increase with the increase of the ampere-turn of the coil. The magnetic field strength will reach the highest value at the junction of the primary and secondary windings, then gradually decrease to zero on the secondary-side winding. the traditional structure has great proximity effect in the windings and has remarkable leakage inductance.

That shown in Fig. 6 (b) is the sandwich structure, the magnetic field strength of the lower winding is half of that of the traditional structure. The structure can significantly reduce the size of the proximity effect and leakage inductance of the winding, and meet the appropriate leakage inductance and winding loss requirements. Those shown in Fig.6 (c) and 6 (d) are the staggered winding method, which can greatly reduce the leakage inductance and winding proximity effect between the primary and secondary windings. That shown in Fig.6 (d) is the non-uniform staggered winding, which can keep magnetic field strength only 1/3 of that for the traditional winding structure, the resultant effect is better than that shown in Fig.6 (c).

In the same manner, by increasing the number of the staggered arrangement and the number of the turns per layer winding, it also can further reduce the intensity of magnetic field winding. However, the increased number of the staggered arrangement will complicate coil winding process and the parasitic capacitor will become larger. As a compromise, fabrication process and cost should be thoroughly considered.

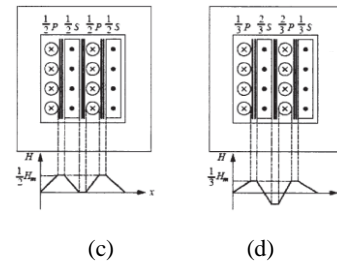
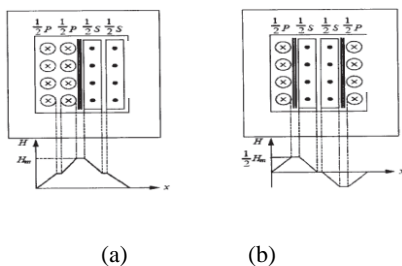


Fig.6 Winding arrangement of power transformer
(a) Traditional structure; (b) Sandwich structure; (c) Uniform staggered structure; (d) Non-uniform staggered

3.4 Wire structure

When current flows through a coil conductor, Coil loss produce ohmic loss, often referred to as the copper loss. At low frequencies, the coil loss can come from the product of DC resistance and RMS current flowing through the coil. But as the frequency increases, the AC loss caused by the skin effect and proximity effect in the winding increases rapidly, and the calculation of AC loss becomes more complicated and need to be performed by means of finite element simulation software. Working frequency, the distance between winding and air gap, the number of distributed air gap, wire AWG and other factors will have a direct impact on the winding loss, and the suitable winding wire can greatly reduce the winding loss. The commonly used wire includes round wire, flat wire, copper foil, stranded wire, as shown in Fig.7. The relationship between the AC resistance and the DC resistance of the wire is shown in Table 2 through the electromagnetic simulation software MAXWELL.

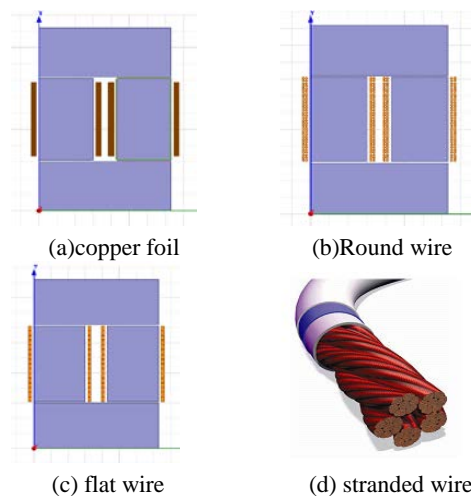


Fig.7 Structure of wire

Stranded wire structure is too complex, and modeling and calculation by simulation is more difficult, so the resistance parameters of the wire should step from the experimental measurement

results instead of from simulation results. Due to its thin diameter and effectiveness against skin effect and proximity effect, stranded wire structure has the feature of least AC loss and has a wide working frequency range. Nevertheless, the relevant process is complex and costly.

Compared with the flat wire, the skin effect of copper foil is smaller under certain conditions of distributed air gap and number of turns, but the proximity effect is obvious. If the number of turns of copper foil is increased, AC losses will rise rapidly. so it is suitable for the design of magnetic components with a low number of turns.

Round wire has the moderate AC loss, simple winding and the low cost, but this is limited by the influence of the maximum wire diameter and skin effect. Flat wire has large AC loss, simple winding and the low cost, but the heat dissipation is poor. After comprehensive assessment, the smoothing reactor is designed by copper foil as a conductor, with moderate cost, low AC loss and good heat dissipation.

4 Design and verification of magnetic components

4.1 Phase shift transformer design

The design procedure of the phase shift transformer is shown in Fig. 8.

The input electrical parameters of the phase-shifting transformer are voltage transfer ratio, rated current, leakage inductance, etc. where voltage level determinate the electrical insulation between the primary and secondary winding distance. The selected structure parameters as variables in the design procedure are the number of turns, magnetic chip width, stack thickness, wire diameter, airway distance, number of airway. Meantime, cabinet installation size limit and temperature rise limit are added to be the boundary condition. Through totally scanning variables, it can arrive at the lowest loss scheme or lowest cost scheme. If taking into account the two goals, the ratio of loss to cost aim should be preset in order to take compromise.

Non-oriented silicon steel sheet, oriented silicon steel sheet, and amorphous alloy can be utilized as magnet core material, and aluminum and copper wire can be used as conductor. They all have an impact on the cost and the loss. Based on the combinations of

three magnetic materials and two kinds of wires, to calculate the weight, the size and the cost of the magnet core, respectively, and to make an analysis and comparison, the results are shown in Table 3. It is evident that amorphous alloy has a huge advantage in terms of the core loss, but the amorphous alloy core lamination coefficient and magnetic saturation is lower than that of the silicon steel sheet. As a result, amorphous alloy transformer leads to large size and high cost.

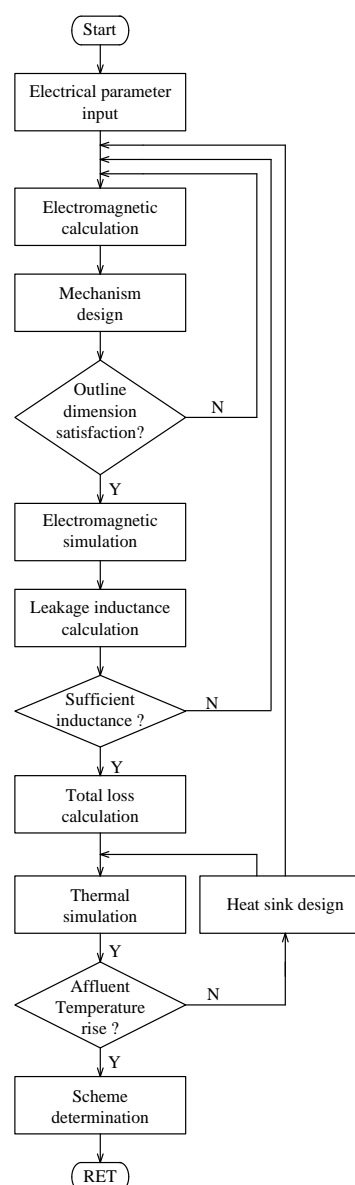


Fig.8 Design procedure of phase shifting transformer

When the oriented silicon steel transformer is compared with non oriented silicon steel sheet transformer, 20% of the cost is in exchange for 10%~15% of the loss and 10%~15% of the volume. When a copper wire transformer is compared with an aluminum transformer, 20% of the cost is in exchange

for less than 5% of loss and 5%~10% of volume. As a comprehensive assessment, aluminum wire and oriented silicon steel sheet phase-shifting transformer become the candidate.

4.2 Smoothing reactor design

The mainly used calculation method of the smoothing reactor is AP method. Due to the presence of the large DC bias, it should be confirmed that the inductance is not reduced at the highest current. In the AP method, when the rated current or maximum current is substituted into the relevant formula, the design error is inevitable. If the substituted is the rated current, the reactor inductance can't meet the requirement of the short-term maximum current. If the substituted is the maximum current, It will lead to over design with large size and high cost. The design flow chart of smoothing reactor is shown in Fig. 9.

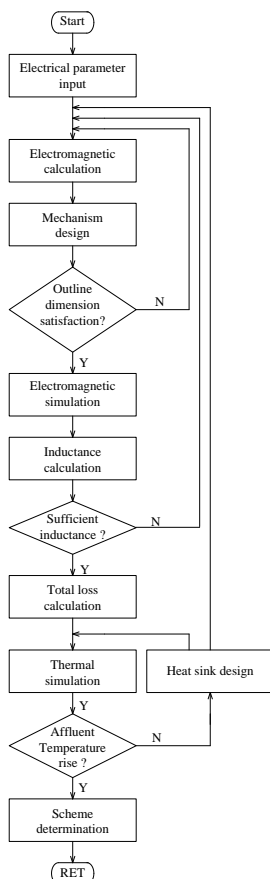


Fig.9 Design flow chart of DC reactor

The input electrical parameters of smoothing reactor are voltage level, maximum current, rated current, ripple current, working frequency, inductance, and so on. The selected structure parameters as variables in the design procedure are the number of turns, wire diameter, magnetic chip width, magnetic

chip thickness, air gap length. Meantime, cabinet installation size limit and temperature rise limit are added to be the boundary condition. Through totally scanning variables, it can arrive at the lowest loss scheme or lowest cost scheme. If taking into account the two goals, the ratio of loss to cost aim should be preset in order to take compromise.

Smoothing reactor inductance is relevant to ripple current magnitude and ripple frequency, and the inductance is in inversely proportion to current ripple amplitude. The following are provided to optimized the design of the smoothing reactor in terms of cutting current ripple coefficient and frequency.

When the operating frequency is kept unchanged, the ripple current is inversely proportional to the inductance of the smoothing reactor. In theory, the smaller the ripple current is, the better the power supply characteristic is. Assuming the working frequency is 10kHz, the relation of the weight, the size, the loss and the cost versus ripple current coefficient is shown in Table 4. The bigger ripple current and the smaller inductance lead to smaller weight, smaller loss and the smaller size. After comprehensive assessment, in order to ensure the stable operation of the DC power supply, proper increase of the ripple current can effectively reduce the weight and volume, loss and cost of the smoothing reactor. The plasma cutting power supply ripple coefficient herein is set as 5%.

When the ripple current amplitude is kept constant, the smoothing reactor inductance is inversely proportional to the working frequency.

If the working frequency is high, the inductance can be reduced, the reactor has the features of small volume but large core loss. The high frequency effect causes more coil loss. If the working frequency is low, the inductance become larger, the reactor has the features of less loss but large size. The high frequency effect causes less coil loss.

When the ripple current amplitude is at 5%, the increase of working frequency can decrease inductance. The relation of the weight, the loss and the size versus the working frequency is shown in Table 5. Obviously, the higher the operating frequency is, the smaller the inductance is, the lighter the smoothing reactor is, the lower the loss is, and the smaller the size of the inductor. The current ripple frequency is relevant to the switching frequency, and the switching frequency is

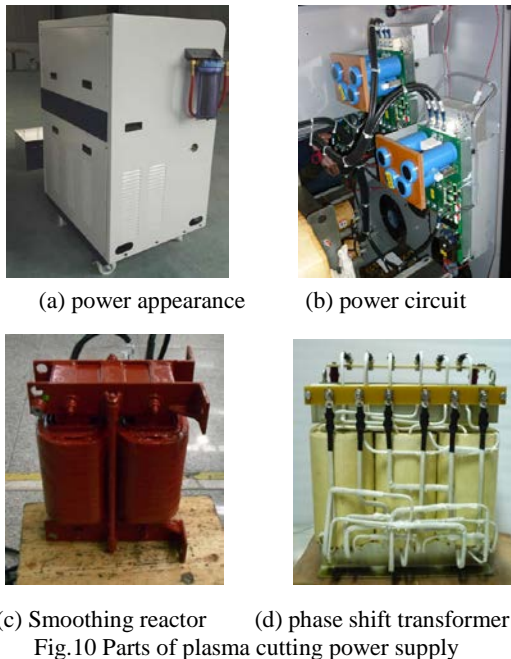
subject to transferred power level (switching loss and on loss), IGBT's switching speed, etc. the proper switching frequency range is 5kHz~20kHz.

Comprehensively evaluated and optimally selected results are listed below: the switching frequency is 20kHz, the inductance is 1.0mH, the weight of coil is 1.6kg, the weight of the magnetic core is 27.1kg, DC loss of the coil is 163.3W, AC loss of the coil 1.7W, the core loss is 32.5W, the size (not including mechanical part) is 156 x 144 x 222mm.

Compared with the 2mH and 10kHz scheme, the total loss is reduced by 37.2%, the total weight is reduced by 29.5% and the overall cost is reduced by 29.2%.

5 Experimental results and analysis

According to the above described optimization design method, the overall plasma cutting power supply is shown in Fig. 10(a), its power circuit in Fig. 10(b), the smoothing reactor in Fig.10(c), and the phase-shifting transformer in Fig.10(d).



Two paralleled Buck DC-DC converters are used as the power circuit of the plasma cutting power supply. The main circuit parameters are listed as follows: the AC input voltage is three-phase 380V, the phase shifting transformer is 380V/(220V+220V), the maximum output DC current of each Buck DC-DC converter is 135A, the total maximum output current 270A, the rated output voltage is 150V, the peak-to-peak value of ripple current is less than 10A at

the maximum load, the switching frequency is 20kHz, the smoothing reactor is 1.0mH, the mains side filtering reactor is 0.5mH, the mains side WYE-connected filtering capacitor is 2.2μF/275V, the electrolytic capacitor is 4*6800 μF/450V. IGBT power module is SKM300GB063D, the driver is HCPL-316J, and the controller is DSP F28335. Three electric fans are used to dissipate out the internal heat, which can lower the ambient temperature of the phase shift transformer, smoothing reactor and IGBT power module.

During the arc-piloting process, the waveforms of output voltage and output current are shown in Fig.11. During the starting process, the waveforms of the output voltage and the output current are shown in Fig.12. During the cutting process, the waveforms of the output voltage and the output current are shown in Fig.13. The electrical test results are satisfactory, proving the overall design is practical and cost-efficient.

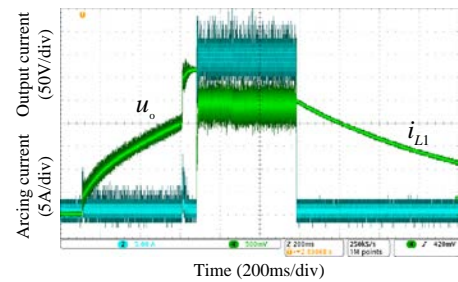


Fig.11 Waveforms of output voltage and output current when arc-piloting

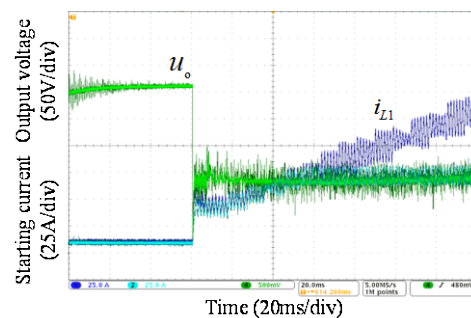


Fig.12 Waveforms of output voltage and starting current when starting

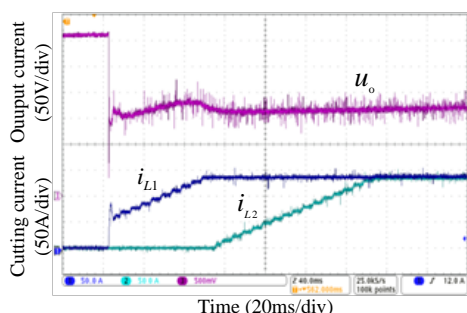


Fig.13 Waveforms of output voltage and output current when cutting

6 Conclusions

On the basis of theoretical analysis of modulation algorithm and control strategy of two Buck DC-DC converters in the chopper type plasma cutting power supply, the optimization design method of smoothing reactor and the phase-shifting transformer are discussed, the design process and experimental results are also given finally. The following conclusions can be drawn: (1) Trapezoidal carrier modulation algorithm and carrier phase shift driving can be used in the two Buck DC-DC converters. The total output current ripple frequency can be multiplied by 4 times at any duty cycle of power switches, which can effectively improve the accuracy of the cutting current and improve the cutting quality; (2) As for the smoothing reactor, in the premise to ensure the ripple current and cutting quality, the switching frequency can be appropriately increased in order to reduce the inductance, the volume and the weight, the optional switching frequency range is 10kHz~20kHz, the inductance is 1.0mH or so. It is an option to design planar inductor, and it can further reduce the copper loss; (3) As for phase shifted transformer, it is needed to comprehensively assess the cost, the size and the power consumption, magnet core material can be thin oriented silicon steel sheet, flat aluminum wire is available, space between winding layers can be reserved for ventilation and heat dissipation.

References

[1] Li Hao. System analysis based on the third generation plasma cutting technology[J]. Ship Standardization Engineer, 2011, 05: 63-68.
 [2] Wang Yong-fei. General situation and application of plasma cutting technology[A]. Sixteenth National Welding Academic Conference Abstracts, 2011, 966-970.
 [3] Wang Lian-zhong, Cui Yong-yuan. Worldwide development

trend of CNC plasma cutting technology[J]. Mechanical workers, 2002, 05: 15-16-21.

- [4] Ma Xue-zhi, Hang Zheng-xiang, Ma Yu-jun, Fu Qin-sheng. Plasma cutting position in the thermal cutting[J]. Journal of Shenyang University of Technology, 1999, 06: 479-481.
 [5] Jia De-li, You Bo, Ren Wei-bo, Zhang Feng-jing, Zhang Xue-yan. Key technology of high power IGBT inverter air plasma cutting power supply[N]. Journal of Harbin University of Science and Technology 2008, 02: 109-112.
 [6] Narongrit Sanajit, Anuwat Jangwanitlert. Improved performance of a plasma cutting machine using a half-bridge dc/dc converter. IEEE International Conference on Robotics and Biomimetics, 2008. Robio 2008, pp. 1601-1606.
 [7] Deng Yu, Zhong He-qing, Lin Lei. Research and development of high power plasma cutting power supply[J]. Electric Welding Machine. 2013, 0917-19. (In Chinese)
 [8] Chen Wei, He Jian-nong. Research content and development trend of high-frequency power electronic device[J]. Advanced technology of electrical engineering and energy. 2000, 02: 30-34. (In Chinese)
 [9] Girish Kamath, Wayne Chin, Norman LeBlanc, Paul Tillman. Planar Tesla coil arc ignition transformer for a plasma cutting power supply. Twenty-Seventh Annual IEEE Applied Power Electronics Conference and Exposition (APEC), 2012, pp. 1027-1033.
 [10] Jia De-li, You Bo, Zhang Feng-jing. Decoupling control based on PID neural network for plasma cutting system. 27th Chinese Control Conference, 2008, pp. 659 - 662.
 [11] He Liang-zong, Duan Shan-xu, Liu Bao-qi, Li Xun, Zhu Guo-rong, Luo Xue-xiao. The IGBT failure mechanism research of DC plasma arc cutting inverter power when arc-starting. IEEE 6th International Power Electronics and Motion Control Conference, 2009. IPEMC'09, pp.1225-1229.
 [12] G R. Kamath. A passive coupled-inductor flying-capacitor lossless snubber circuit for plasma cutting power supply. Twentieth Annual IEEE Applied Power Electronics Conference and Exposition, 2005. APEC 2005. Vol. 1, pp. 237-243.
 [13] Chas. Proteus Steinmetz. On the law of hysteresis[J]. Proc. IEEE. 1984, 72 (2): 197-221.
 [14] J. Jin. The Finite Element Method in Electromagnetics[K]. John Wiley Inc, 1993: 45-54.
 [15] Boyce. Elementary Differential Equations and Boundary Value Problems[K]. John Wiley Sons Inc, 1977: 43-47.
 [16] P. L. Dowell. Effects of eddy currents in transformer windings[C]. PROC. IEE. 1966, 113(8): 1387-1394.
 [17] Frederic Rovert, Pierre Mathys, Bruno Velaerts, and Jean-Pierre Schauwers. Two-Dimensional Analysis of the Edge Effect Field and losses in High-Frequency Transformer Foils[J]. IEEE. 2005, 41(8): 2377-2383.
 [18] Roshen W.Gao Lei. Study on the output voltage unbalance and its influence on multiphase rectification transformer[D]. Harbin: Harbin Institute of Technology, 2012. (In Chinese)
 [19] G Bertotti. General properties of power losses in soft ferromagnetic materials[J]. IEEE Trans. Magn. 1988. 24(1): 621-630.
 [20] Boglietti, A. Cavagnino, M. Lazzari, and M. Pastorelli. Predicting iron losses in soft magnetic materials with

arbitrary voltage supply: An engineering approach[J]. IEEE Trans. Magn.2003.39(2): 981-989.

[21] J. D. Lavers, P. P. Biringer. Prediction of core losses for high flux densities and distorted flux waveforms[J]. IEEE Trans. on Mag. 1976.12(6): 1053-1055.

[22] Reinert J, Brockmeyer A, De Doncker, et al. Calculation of Losses in Ferro and Ferrimagnetic Materials based on the Modified Steinmetz Equation [J]. IEEE Trans. on Industry Applications.2001.37(4): 1055-1061.

[23] Ferreira J. A. Improved analytical modeling of conductive losses in magnetic components[J]. IEEE Trans. on Power Electronics, 1994, 9(1): 127-131.

[24] Ferreira J. A. Appropriate modeling of conductive losses in the design of magnetic components[C]. in Proc. IEEE PESC, San Antonio, USA, 1990: 780-785.

[25] Girish Kamath, Wayne Chin, Norman LeBlanc, Paul Tillman. Forced air cooled quasi-planar 60A, 600μH inductor for a plasma cutting power supply. 2012 Twenty-Seventh Annual IEEE Applied Power Electronics Conference and Exposition (APEC), pp.1747 -1753, 2012.

Table 1 Comparison of magnet core materials and structures

Structure	High permeability magnetic material with air gap	Magnetic powder core	Magnetic material mixed with high and low permeability	Magnetic material with high permeability and air gap
Volume	Low	Large	Medium	Low
Cost	Low	Medium	Medium	Vast
Loss	Medium	Medium	Low	Large
Inductance	Linear	Non-linear	Non-linear	Linear

Table 2 Relationship between AC resistance and DC resistance of conductor

Conductor	DC loss (W)	AC loss (W)	Total loss (W)	Rac/Rdc
Copper foil	296.3	2.6	298.9	28.4
Round wire	298.9	6.5	305.4	69.4
Flat wire	289.0	13.7	302.7	152.1
Stranded wire	293.4	0.9	294.3	10 (Estimated)

Table 3 Scheme Comparison of aluminum and copper wire phase shifting transformer

Wire material		Aluminium wire			Copper wire		
Core material	Wire material	Non oriented silicon steel sheet	Oriented silicon steel sheet	Amorphous alloy	Non oriented silicon steel sheet	Oriented silicon steel sheet	Amorphous alloy
Weight(kg)	Coil	45	42	48	57	53	85
	Core	191	143	169	204	158	154
	Total	286	231	264	319	253	286
Loss(W)	Coil	1422	1340	1535	1397	1361	1618
	Core	300	143	28	278	146	23
	Total	1723	1483	1562	1675	1507	1641
Size (mm)		580×410×590	550×410×560	610×430×600	550×440×550	520×410×530	570×410×590
Copper and iron cost (RMB)		3403	4092	12584	4081	4858	13475

Table4 Scheme comparison of fixed working frequency

Current ripple factor	Inductance (mH)	Winding weight(kg)	Magnet core weight (kg)	Total weight(kg)	Winding loss (W)	Magnet core loss (W)	Total loss (W)	Outline dimension (mm)
0.5%	20	10.4	512.7	523.2	1046.3	0.3	1046.6	416×404×498

1.0%	10	6.5	264.1	270.7	655.7	6.8	662.4	328×342×384
2.0%	5.0	4.3	133.0	137.3	433.2	11.4	444.6	242×302×305
3.0%	3.33	3.8	72.2	76.0	387.1	12.6	399.7	182×288×245
5.0%	2.0	3.0	37.7	40.7	298.9	16.0	314.9	164×196×224

Table 5 Scheme comparison of fixed ripple current coefficient

Frequency (kHz)	Inductance (mH)	Weight of coil (kg)	Weight of mag. core (kg)	Total weight (kg)	Loss of coil (W)	Loss of mag. core (W)	Total loss (W)	Outline (mm)
5.0	4.0	4.2	87.7	91.9	422.3	13.1	435.3	204×285×262
7.5	2.67	3.3	57.8	61.1	331.1	25.2	356.3	182×234×242
10.0	2.0	3.0	37.7	40.7	298.9	16.0	314.9	164×196×224
12.5	1.6	2.4	36.8	39.1	238.3	21.9	260.2	160×191×222
15.0	1.33	2.0	35.9	37.8	197.7	28.8	226.6	156×186×222
17.5	1.14	1.8	30.9	32.6	179.0	36.2	215.2	156×162×222
20.0	1.0	1.6	27.1	28.7	165.0	32.5	197.5	156×144×222
22.5	0.89	1.6	21.2	22.8	163.8	30.6	194.4	148×130×222
25.0	0.8	1.5	19.1	20.7	154.4	32.2	186.6	148×119×222